Pharmaceutical Research, Vol. 26, No. 2, February 2009 (© 2008)
DOI: 10.1007/s11095-008-9739-4

Research Paper

Pharmacokinetic and Pharmacodynamic Modeling of a Humanized Anti-IL-13 Antibody in Naive and Ascaris-Challenged Cynomolgus Monkeys

Yulia Vugmeyster,[1,3] Xianbin Tian,[1] Pamela Szklut,[1] Marion Kasaian,[2] and Xin Xu[1]

Received May 16, 2008; accepted September 25, 2008; published online October 31, 2008

Purpose. Neutralization of IL-13 is an attractive approach for treatment of asthma. In this report, we developed a novel PK–PD model that described the relationship between the circulating concentrations of total IL-13 and a neutralizing anti-IL-13 antibody (Ab-02) in the model of acute airway inflammation induced by Ascaris challenge to cynomolgus monkeys, as well as in naive monkeys.
Methods. Cynomolgus monkeys were administered a single intravenous or subcutaneous dose of Ab-02. Total IL-13 and Ab-02 concentrations were measured by immunoassays.
Results. Modeling and simulations indicated that: (1) Ascaris challenge induced ~ three-fold increase in circulating IL-13 concentrations, when compared to naive animals, consistent with the notion that Ascaris-induced airway inflammation was IL-13-mediated; (2) the transient increase in total IL-13 concentrations observed in both naive and Ascaris-challenged monkeys following Ab-02 administration was due to the increase in Ab-02-bound IL-13, while free IL-13 was decreased; and (3) the extent and duration of neutralization of circulating IL-13 were different in naive and Ascaris-challenged monkeys for the same Ab-02 dose regimen.
Conclusions. The PK–PD model presented in this report may be applied to study drug–ligand interactions when a free ligand cannot be directly assayed but total ligand concentrations are modulated by the drug administration.

KEY WORDS: Asthma; IL-13; Monoclonal antibody; Pharmacodynamics; Pharmacokinetics.

INTRODUCTION

Cytokine neutralization by monoclonal antibodies or cytokine receptor/Fc fusion proteins is being explored as a potential therapeutic approach for a variety of cytokine-mediated disorders, including autoimmune diseases, such as rheumatoid arthritis (RA), asthma, and systemic lupus erythematosus (SLE) (1–4). A common problem in the development of therapeutic proteins is that cytokine neutralization cannot be directly monitored in the presence of a drug, due to unavailability of an assay method of sufficient sensitivity to measure free cytokine concentrations. Instead, total (free plus drug-bound) cytokine concentrations are often used as a surrogate pharmacodynamic (PD) marker of drug activity. There are several examples of anti-cytokine proteins acting as "cytokine traps", resulting in increased total circulating cytokine concentrations following drug administration, presumably due to slower elimination of a drug-bound circulating cytokine, compared to that of a free circulating cytokine (5–7).

When free cytokine concentrations (in the presence and often in the absence of an anti-cytokine protein) cannot be directly assayed, PK–PD modeling could be a useful tool for delineating a relationship between the kinetics of ligand neutralization and the concentration-time profile of an anti-cytokine therapeutic, using total cytokine concentrations as a PD marker. These models may be especially useful when data from both healthy and disease subjects (animals or humans) are available, so that the free cytokine concentrations can be estimated by modeling before and after therapy in both settings. Establishing a relationship between the kinetics of ligand neutralization and the concentration-time profile of a potential therapeutic, combined with efficacy data, could be useful for design of an optimal dosing regimen in animal pharmacology or in clinical studies.

In this report, we establish an integrated model that describes pharmacokinetics and pharmacodynamics of an anti-IL-13 (interleukin-13) antibody in both naive animals and in the animal pharmacology study. The model is used to characterize the kinetics of IL-13 neutralization by an anti-IL-13 antibody in both naive and pharmacology study settings.

Neutralization of IL-13 is an attractive approach for therapeutic intervention in asthma, as this Th2 cytokine plays an important role in asthma pathogenesis in animal models of asthma (8–13). In addition, there are consistent correlations between polymorphism in the IL-13 gene and asthma susceptibility in humans (14). Neutralization of IL-13 with anti-IL-13 antibodies or with IL-13 receptor α2/Fc fusion protein (IL-13Rα2-Fc) prevents airway hyperresponsiveness and other asthmatic changes in mice (11,13,15–17), sheep (18), and cynomolgus monkeys (18,19).

[1] Department of Drug Safety and Metabolism, Wyeth Research, One Burtt Road, Andover, MA 01810, USA.
[2] Department of Discovery, Wyeth Research, Cambridge, MA, USA.
[3] To whom correspondence should be addressed. (e-mail: yvugmeyster@wyeth.com)

IL-13 signals *via* a receptor complex consisting of IL-13 receptor α1 (IL-13Rα1) and interleukin-4 receptor alpha (IL-4Rα) subunits (8,9). IL-13 first undergoes a low affinity interaction with IL-13Rα1, which recruits IL-4Rα to form an active signaling complex with high affinity for IL-13, leading to phosphorylation of STAT6 and downstream cellular activation events.

Ab-02 is a humanized anti-IL-13 antibody that blocks binding of IL-13Rα1 to human and non-human primate IL-13 (19,20). Ab-02 does not cross-react with either rodent or sheep IL-13; thus non-human primates are used as pharmacological species. Ab-02 has been shown to be efficacious (at 10 mg/kg IV dose) in the model of acute airway inflammation induced by Ascaris challenge in cynomolgus monkeys (19). In this study, the Ab-02 (PK) and total IL-13 (PD) serum concentration data following Ab-02 administration to naive and Ascaris-challenged monkeys were used to establish an integrated PK-PD model and characterize the kinetics of serum IL-13 neutralization.

MATERIALS AND METHODS

Test Article

Murine Ab-02 was cloned from BALB/c mice immunized with the N-terminal 19 amino acids of non-human primate IL-13. The humanized version of this antibody, Ab-02 (IgG1, k), was described previously and generated at Wyeth Research (Cambridge, MA) (19,20).

Study Design and Sample Collection

Study design is summarized in Table I. Single dose pharmacokinetic studies in protein-free adult cynomolgus monkeys were conducted at Wyeth Research (Pearl River, NY and Andover, MA for Study 1 and Study 2, respectively), as previously described (19,20). Ab-02 was administered by intravenous (IV) injection into saphenous vein or by subcutaneous (SC) route. Blood samples were collected into serum separator tubes at the designated time-points (Table I), allowed to clot at room temperature for approximately 15 min, and processed for serum by centrifugation (~11,000 rpm for 10 min).

The Ascaris-challenge study protocol was described previously (18). In brief, several months prior to the study untreated monkeys were given an initial screening challenge with Ascaris suum antigen. Monkeys that responded with at least a two-fold increase in bronchoalveolar lavage (BAL) eosinophil content 24 h post-challenge were selected for the study. Animals were administered either Ab-02 (10 mg/kg) or a negative control (10 mg/kg of carimune NH immune globulin intravenous (IVIG); ZLB Bioplasma Inc., Berne, Switzerland) by the IV route and were challenged with 0.75 μg Ascaris suum antigen (obtained from Greer Diagnostics, Lenoir, NC and reconstituted with PBS) 24 h post administration of Ab-02 or a negative control.

All aspects of these studies adhered to the "Principles of Laboratory Animal Care" and were approved by the Wyeth Institutional Animal Care and Use Committee.

Quantitation of Ab-02 and Total IL-13 Concentration in Serum

The concentrations of Ab-02 in serum samples were determined using a quantitative enzyme-linked immunosorbent assay (ELISA). In this assay, the recombinant human IL-13 ligand, which contains a FLAG octapeptide fusion tag (Asp-Tyr-Lys-Asp-Asp-Asp-Asp-Lys) was captured onto a microtiter plate by an anti-FLAG monoclonal antibody. After blocking and washing, the serum samples containing Ab-02 or the Ab-02 standards were incubated on the plate to allow for binding to the IL-13. Bound Ab-02 was detected with a mouse anti-human IgG (Fc) antibody conjugated to horseradish peroxidase (HRP). The enzyme substrate 2,2′ azino-di (3-ethyl-benzthiazoline-6-sulfonate) (ABTS) was added and optical densities were measured at 405 nm. The lower limit of quantitation of the assay was approximately 10.5 ng/mL and acceptable %CV was ≤20%.

The concentrations of total IL-13 in serum samples obtained from Ab-02-treated monkeys were determined using a quantitative ELISA. In this assay, an anti-IL-13 antibody (Ab-01, Wyeth Research) that was able to bind IL-13 in the presence of Ab-02 was used as a capture. After blocking and washing, the serum samples containing IL-13 from *in vivo* studies or the non-human primate IL-13 standards were incubated on the plate to allow for binding to the anti-IL-13 capture antibody. Total IL-13 was detected with a biotinylated Jin2, an anti-IL-13 antibody that binds to an IL-13 epitope that is distinct from those of Ab-01 and Ab-02. Streptavidin conjugated to HRP and the enzyme substrate 3,3′,5,5′-tetramethylbenzidine (TMB) peroxidase were added and optical densities were measured at 450 nm. The low limit of quantitation of the assay was approximately 0.15 ng/mL and acceptable %CV was ≤20%.

Pharmacokinetic and Pharmacodynamic Modeling and Simulations

An integrated pharmacokinetic and pharmacodynamic model that described the relationship between observed

Table I. Study Design

Study number	*N*, sex	Ab-02 dose (mg/kg)	Dosing volume and buffer	PK and PD sampling time-points (days)
Study 1, naive monkeys	3, males	1 (IV) and 2 (SC)	1 mL/kg in histidine–sucrose buffer[b]	0, 0.004, 0.042,0.125, 0.25, 1, 2, 3, 5, 7, 14, 20, 28, 35, 42
Study 2, Ascaris-challenged monkeys[a]	8, males	10 (IV)	2–3 mL/kg in PBS	0, 1, 2, 8, 15, 36, 57, 85, 113

[a] Animals were challenged with 0.75 μg *Ascaris suum* 24 h post Ab-02 administration
[b] 10 mM histidine, 5% sucrose, pH 6.0

serum concentrations of Ab-02 and total IL-13 was developed using WinNonlin software V 5.1.1(Pharsight, Mountain View, CA) (Fig. 1). The pharmacokinetics of Ab-02 was described with a two-compartmental model including a central compartment (C_{Ab}; V) and a peripheral compartment ($C_{2,Ab}$; V_2). $CL_{d,Ab}$ represented the distribution clearance between these two compartments. Clearance (CL_{Ab}) of Ab-02 was assumed only through the central compartment. The pharmacodynamics of Ab-02 was characterized with the neutralization of endogenous IL-13. Based on the bivalent feature of IgG, the model assumed that each Ab-02 molecule had two independent binding sites for IL-13 with identical association (k_{on}) and disassociation (k_{off}) rate constants. k_{on} was a second order rate constant governing the formation of Ab-02/IL-13 (Ab–IL-13) complex and k_{off} was a first order rate constant governing the disassociation of Ab–IL-13 complex. $CL_{complex}$ represented the serum clearance of Ab–IL-13 complex. Furthermore, non-cooperative binding for the two IgG binding sites was assumed, so that k_{on} and k_{off} rate constants were assumed to be identical for the first and the second binding steps. The homeostasis of IL-13 was assumed to be regulated by IL-13 production (zero order, $k_{syn,}$) and degradation ($CL_{IL\text{-}13}$). Differential equations derived from the model scheme in Fig. 1 are as follows:

$$\begin{aligned} dC_{Ab}/dt = {} & [In(t) + CL_{d,Ab} \bullet C_{2,Ab} - (CL_{d,Ab} + CL_{Ab}) \bullet C_{Ab}]/V \\ & - k_{on} \bullet C_{Ab} \bullet (C_{IL-13} - C_{Ab-(IL-13)} - C_{Ab-(IL-13)_2}) + k_{off} \bullet C_{Ab-(IL-13)} \\ & \text{when } t = 0, C^0_{Ab} = In(t)/V \end{aligned} \quad (1)$$

$$\begin{aligned} dC_{2,Ab}/dt = {} & (CL_{d,Ab} \bullet C_{Ab} - CL_{d,Ab} \bullet C_{2,Ab})/V_2 \\ & \text{when } t = 0, C^0_{2,Ab} = 0 \end{aligned} \quad (2)$$

$$\begin{aligned} dC_{Ab-(IL-13)}/dt = {} & k_{on} \bullet C_{Ab} \bullet (C_{IL-13} - C_{Ab-(IL-13)} - C_{Ab-(IL-13)_2}) \\ & - CL_{complex} \bullet C_{Ab-(IL-13)} - k_{off} \bullet C_{Ab-(IL-13)} + k_{off} \bullet C_{Ab-(IL-13)_2} \\ & - k_{on} \bullet C_{Ab-(IL-13)} \bullet (C_{IL-13} - C_{Ab-(IL-13)} - C_{Ab-(IL-13)_2}) \\ & \text{when } t = 0, C^0_{Ab-(IL-13)} = 0 \end{aligned} \quad (3)$$

$$\begin{aligned} dC_{Ab-(IL-13)_2}/dt = {} & k_{on} \bullet C_{Ab-(IL-13)} \bullet (C_{IL-13} - C_{Ab-(IL-13)} - C_{Ab-(IL-13)_2}) \\ & - CL_{complex} \bullet C_{Ab-(IL-13)_2} - k_{off} \bullet C_{Ab-(IL-13)_2} \\ & \text{when } t = 0, C^0_{Ab-(IL-13)_2} = 0 \end{aligned} \quad (4)$$

$$\begin{aligned} dC_{IL-13}/dt = {} & [k_{syn} - CL_{IL-13} \bullet (C_{IL-13} - C_{Ab-(IL-13)} - C_{Ab-(IL-13)_2})]/V \\ & - k_{on} \bullet C_{Ab} \bullet (C_{IL-13} - C_{Ab-(IL-13)} - C_{Ab-(IL-13)_2}) \\ & - k_{on} \bullet C_{Ab-(IL-13)} \bullet (C_{IL-13} - C_{Ab-(IL-13)} - C_{Ab-(IL-13)_2}) \\ & + k_{off} \bullet C_{Ab-(IL-13)} + k_{off} \bullet C_{Ab-(IL-13)_2} \\ & \text{when } t = 0, C^0_{IL-13} = k_{syn}/CL_{IL-13} \end{aligned} \quad (5)$$

$$\begin{aligned} & \text{For iv bolus dose :} \\ & In(t) = Dose \end{aligned} \quad (6)$$

$$\begin{aligned} & \text{For sc dose :} \\ & In(t) = k_a \bullet F \bullet Dose \end{aligned} \quad (7)$$

Since preliminary modeling indicated that the Ab-02, IL-13, and Ab–IL-13 complex had similar estimates of volume of distribution in a central compartment (~0.1–0.3 L), a single volume variable (V) was used in the final modeling for model parsimony. A 1st order absorption rate constant (k_a) was used to describe the absorption process for a subcutaneous dose.

Except for the estimate of bioavailability (F), PK-PD parameter estimates were obtained by simultaneously fitting the model to both serum Ab-02 and total IL-13 concentration-time profiles from either individual naive or Ascaris-challenged monkeys. The integrated PK-PD model was fitted first to data from naive monkeys with IV (n=3) and SC (n=3) doses to obtain model parameter estimates (such as $CL_{d,Ab}$, CL_{Ab}, $CL_{complex}$, $CL_{IL\text{-}13}$, k_{syn}, k_{on}, k_{off}, V, and V_2) for each monkey. Bioavailability (F) of the anti-IL-13 antibody after the SC dose was estimated previously with non-compartmental analysis (20). One naive monkey (Monkey #5) in the SC arm of the study, had a sharp decline in Ab-02 concentrations in the terminal phase (and a faster drop of total IL-13 concentrations), compared to other naive monkeys in both the IV and SC arms (Fig. 2A), likely due to formation of anti-Ab-02 antibodies. Therefore Monkey #5 was excluded from the calculation of the mean model parameters in the naive-

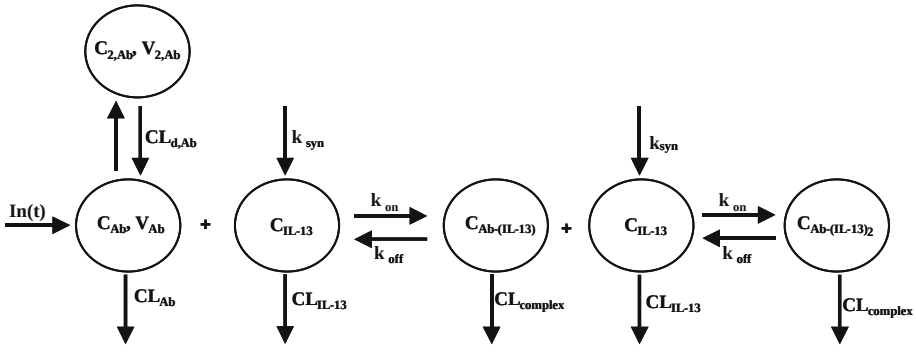

Fig. 1. Schematic representation of PK–PD model of Ab-02. Ab is Ab-02. Complex is Ab-02/IL-13 complex. $CL_{d,Ab}$ and CL_{Ab} are distribution clearance and serum clearance of Ab-02, respectively. $CL_{complex}$ and $CL_{IL\text{-}13}$ are serum clearance of the complex and IL-13, respectively. k_{syn} is a zero-order IL-13 synthesis rate constant, k_{on} is a second-order association rate constant, and k_{off} is a first-order dissociation rate constant. V and V_2 are volumes of distribution of Ab-02 in the serum (*central*) and the second compartment, respectively.

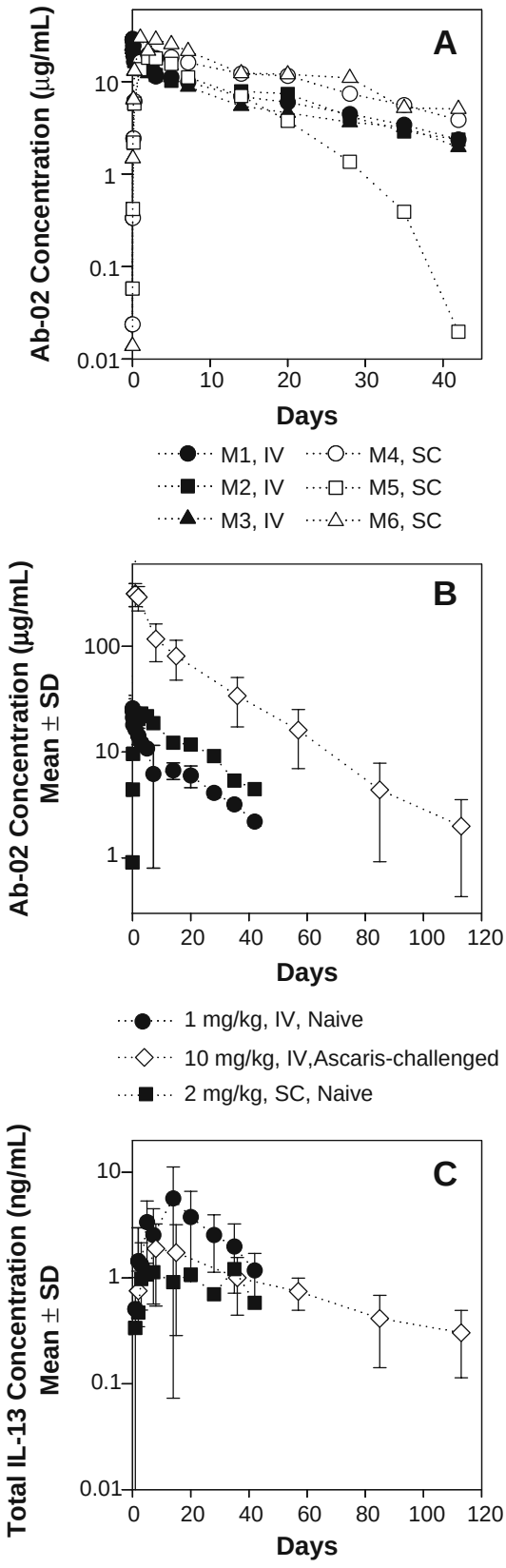

Fig. 2. Ab-02 and total IL-13 concentration-time profiles in cynomolgus monkeys. A single 1 mg/kg IV or 2 mg/kg SC dosage of Ab-02 was administered to naive cynomolgus monkey and a single 10 mg/kg IV dosage of Ab-02 was given to Ascaris-challenged cynomolgus monkeys. The challenge was performed with 0.75 μg of Ascaris suum antigen 24 h post administration of the Ab-02. Ab-02 (**A**, **B**) and total IL-13 (**C**) concentrations were determined using quantitative ELISAs. Data points show individual animal values (**A**) or mean values (**B** and **C**). For the mean values, $N=3$ for 1 mg/kg IV group, $N=2$ for 2 mg/kg SC group, and $N=8$ for 10 mg/kg IV group, with Monkey #5 in the SC group being excluded from calculations of the mean values. *Error bars* indicated standard deviation from the mean values. *M* = monkey.

model settings. It was assumed that k_{on} and k_{off} were not altered by Ascaris challenge. Therefore, mean k_{on} and k_{off} estimates obtained from naive monkeys were used in the model fitting for Ascaris-challenged monkeys to obtain model parameter estimates (such as $CL_{d,Ab}$, CL_{Ab}, $CL_{complex}$, CL_{IL-13}, k_{syn}, V, and V_2) for each monkey. The onset of inflammation in Ascaris-challenged monkeys was assumed to occur instantaneously after the challenge at 24 h post dose. Thus, naive condition was assumed for Ascaris-challenged monkeys in the pre-challenge period (0–24 h) by fitting the data with mean parameters obtained from naive monkeys. All data were reported as mean ± SD ($n=5$ for naive and $n=8$ for Ascaris-challenged monkeys). Statistical significance ($p<0.05$) was assessed with unpaired Student *t*-test.

Simulations for concentrations of Ab-02, total IL-13, and free (unbound) IL-13 in naive or Ascaris-challenge settings after different dose regimens of Ab-02, were conducted with the corresponding mean parameters obtained from PK-PD modeling. When Ascaris challenge was assumed at Day 1 (as used in the experiment design of Study 2), simulations for the 0–24 h period were performed with mean parameter estimates from naive settings, while simulations for Day 1 onward were performed with mean parameter estimates from the Ascaris-challenge settings. When Ascaris challenge was assumed at Day 0 (for a hypothetic "established inflammation" situation), simulations for all time-points were performed with mean parameter estimates from the Ascaris-challenge settings.

RESULTS

PK and PD Profiles in Naive and Ascaris-Challenged Monkeys

Mean concentration-time profiles of Ab-02 (1 mg/kg, IV and 2 mg/kg SC, Study 1) in naive cynomolgus monkeys were reported previously (20). Individual concentration-time profiles of Ab-02 in Study 1 are shown in Fig. 2A. A sharp decline of Ab-02 serum concentrations after ~14 days post-dose was observed in one animal (Monkey #5) in the SC arm of the study, relative to other five animals (three in the IV arm and two in the SC arm) in Study 1. Mean concentration-time profiles of Ab-02 in Ascaris-challenged monkeys (10 mg/kg, IV, with Ascaris challenge 24 h post-dose, Study 2) together with those in naive monkeys are summarized in Fig. 2B.

Quantitative ELISA were developed to measure total IL-13 concentrations in the absence or presence of Ab-02. Serum IL-13 concentrations were undetectable by these assays in pre-dose samples or in all samples from control animals treated with IVIG (data not shown). After Ab-02 administration, total IL-13 concentrations were transiently increased in both Study 1 (naive monkeys; 1 mg/kg IV or 2 mg/kg SC) and in Study 2 (10 mg/kg IV, with Ascaris challenge 24 h post-dose) (Fig. 2C). There was high inter-animal variability in the concentration-time profiles of total

IL-13. Monkey #5 in the SC arm of Study 1 had an apparent sharp decline in the total IL-13 concentrations, compared to other five naive monkeys on Study 1 that were treated with Ab-02, likely due to formation of anti-Ab-02 antibodies in this animal. The onset of decline in total IL-13 in Monkey #5 coincided with that in Ab-02 concentrations in this monkey (data not shown).

Results of the previously reported cell-based assay performed with sera from Ascaris-challenged animals indicated that samples with detectable concentrations of total IL-13 had no IL-13-mediated biological activity (19), suggesting that the transient increase in total IL-13 concentrations in naive and Ascaris-challenged monkeys was due to the increase in Ab-02-bound IL-13. However, the concentration-time profile of free (biologically active) IL-13 following Ab-02 administration to naive or Ascaris-challenged animals remained to be characterized.

PK–PD Modeling

An integrated drug–ligand binding PK–PD model depicted in Fig. 1 was developed to describe the relationship between the observed total serum concentrations of IL-13 and Ab-02 in naive and Ascaris-challenged monkeys. In this model, the pharmacokinetics of Ab-02 was described with a two-compartmental model and the pharmacodynamics of Ab-02 was characterized with the neutralization of endogenous IL-13. Based on the bivalent feature of IgG and monovalent feature of the antigen (IL-13), the models were developed under the assumption that Ab-02 can bind either one or two IL-13 molecules, in a sequential manner. Furthermore, non-cooperative binding for the two IgG binding sites was assumed, so that k_{on} and k_{off} rate constants were assumed to be identical for the first and the second binding steps. The homeostasis of IL-13 was assumed to be regulated by the zero-order synthesis (k_{syn}) and degradation (CL_{IL-13}) of IL-13. For PK–PD modeling, raw concentration data (measured in ng/mL or μg/mL) was converted to nM units, using molecular weights of 150 and 10 kDa for Ab-02 and IL-13 respectively.

In general, this model adequately characterized the animal data (Figs. 3 and 4; and Table II). The residuals were evenly distributed, without noticeable systematic bias (Fig. 3). The representative fittings for each of the three dose groups (naive monkey, 1 mg/kg IV, Study 1; naive monkey, 2 mg/kg SC, Study 1; and Ascaris-challenged monkey, 10 mg/kg IV, Study 2) are shown in Fig. 4. It should be noted that the sharp decline of both Ab-02 and total IL-13 serum concentrations in Monkey #5 from the SC arm of Study 1 could not be described by this integrated PK-PD model. Therefore, the PK parameters from Monkey #5 were excluded from the calculation of the mean model parameters in the naive-animal settings.

PK and PD parameters generated from the model fitting for both naive and Ascaris-challenged monkeys are summarized in Table II. The clearance of unbound Ab-02 (CL_{Ab}) from the central compartment was low (~0.013–0.015 L/day) and was similar between the naive and Ascaris-challenged monkeys. In naive animals, the clearance of Ab-02/IL-13 complex from the central compartment ($CL_{complex}$) was ~5–6 fold lower, compared to CL_{Ab}. In Ascaris-challenged animals,

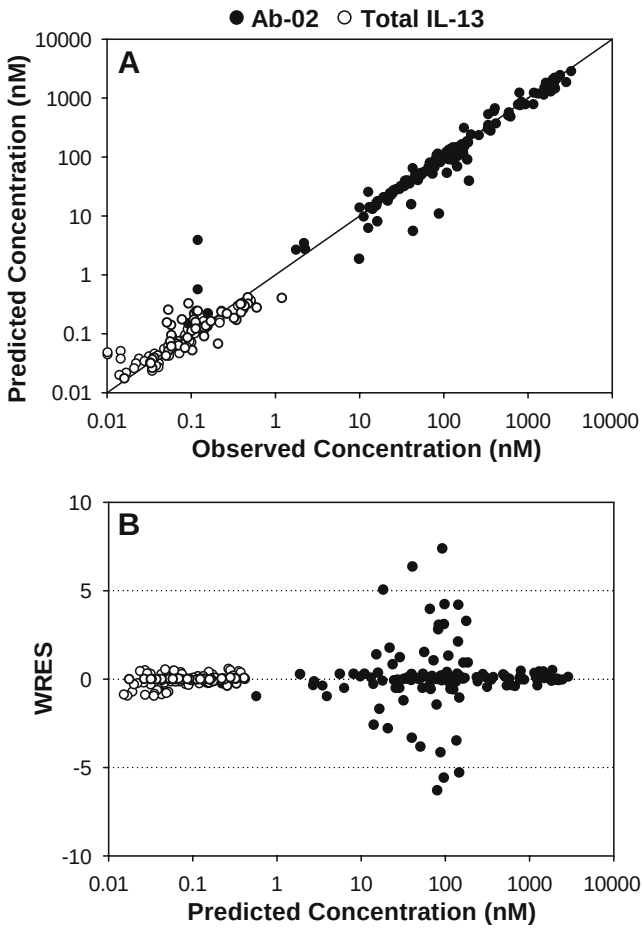

Fig. 3. Goodness-of-fit plots. Ab-02 (*closed circle*) and total IL-13 (*open circle*) concentrations following a single dosage of Ab-02 were fitted using the integrated PK–PD model depicted in Fig. 1. Individual observed *versus* individual predicted concentrations based on model fittings (**A**) and individual weighted residuals (WRES) *versus* individual predicted concentrations based on model fittings (**B**) following a single dosage of Ab-02 are shown for five naive (N=3, 1 mg/kg IV and N=2, 2 mg/kg SC) and eight Ascaris-challenged cynomolgus monkeys (10 mg/kg, IV). One animal (Monkey #5) in the SC group was excluded from these analyses due to a sharp decline in Ab-02 and total IL-13 concentrations in the terminal phase, compared to other naive monkeys in the study.

$CL_{complex}$ was similar to CL_{Ab}. Thus, $CL_{complex}$ was ~ 5-fold higher in Ascaris-challenged animals, when compared to that in naive monkeys. The volume of Ab-02 in the central compartment (V) was found to be in the range of the typical plasma volume in cynomolgus monkeys for both naive and Ascaris-challenged animals. However, V and the distribution clearance of Ab-02 ($CL_{d,Ab}$) were significantly lower in the Ascaris-challenged monkeys, when compared to that in naive monkeys. This result is in accord with the lower estimate for the volume of distribution in Ascaris-challenged monkeys obtained with earlier non-compartment analysis (20).

The neutralization of IL-13 was governed by k_{on} and k_{off}, the rate constants of the coupling/uncoupling of Ab-02 and free IL-13. The mean k_{on} and k_{off} estimates were 0.0896 $nM^{-1}day^{-1}$ and 0.1630 day^{-1}, respectively. Baseline IL-13 concentrations were defined by the ratio of endogenous IL-13 synthesis rate (k_{syn}) and the clearance of IL-13 from the

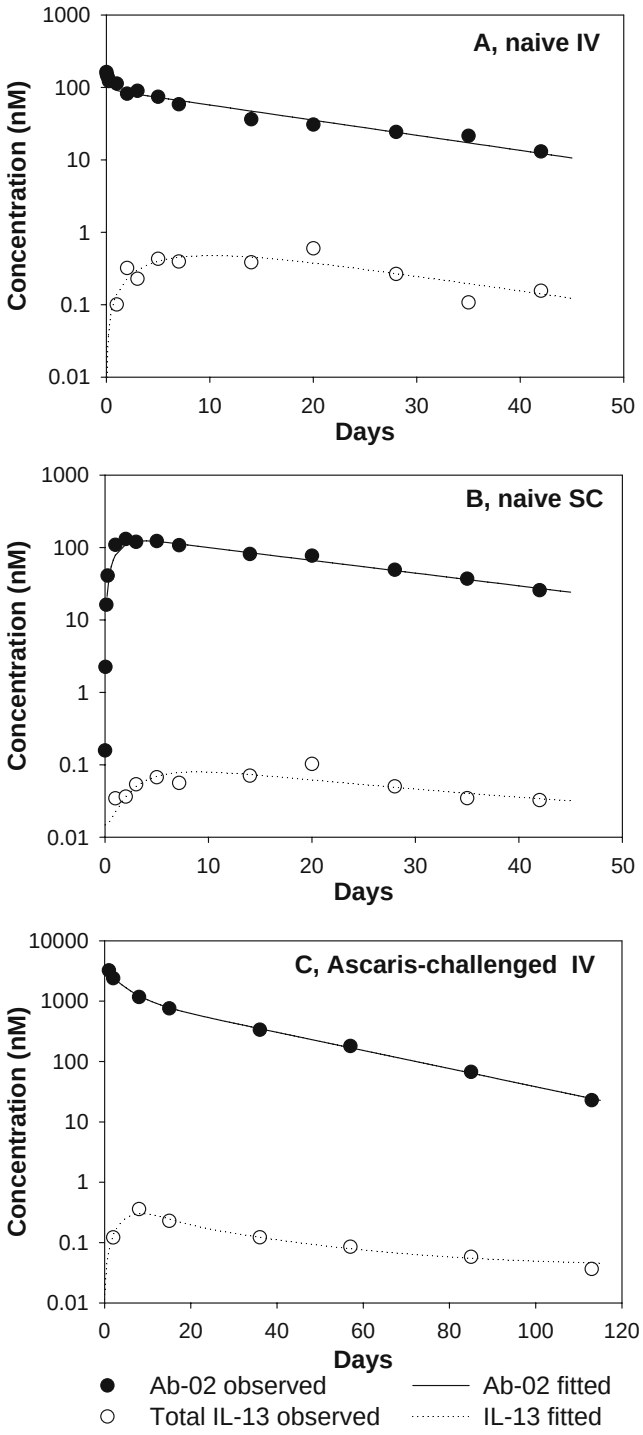

Fig. 4. Representative individual animal fittings. Ab-02 (*closed circle*) and total IL-13 (*open circle*) concentrations following a single dosage of Ab-02 were fitted using the integrated PK–PD model depicted in Fig. 1. Representative individual fits are shown for each of the three dose groups: naive, 1 mg/kg IV, Study 1 (**A**); naive, 2 mg/kg SC, Study 1 (**B**); and Ascaris-challenged, 10 mg/kg IV, Study 2 (**C**). Observed Ab-02 and total IL-13 concentrations are shown by *closed and open circles*, respectively. Fitted Ab-02 and total IL-13 concentrations are shown by *solid line and dotted lines*, respectively.

central compartment ($CL_{IL\text{-}13}$) (21–23). The estimated baseline IL-13 concentration was ~0.0115 nM in naive monkeys and it was ~3-fold higher (~0.0346 nM) in Ascaris-challenged monkeys ($p<0.001$).

Prediction of Free IL-13 Concentrations

Simulations based on the mean parameter estimates of the integrated PK-PD model were performed to predict the concentrations of free and Ab-02-bound IL-13 post Ab-02 administration. These simulations predicted that the transient increase in total IL-13 concentrations in both Study 1 (naive) and Study 2 (Ascaris-challenged at Day 1) was due to the increase in Ab-02-bound IL-13, while free IL-13 was decreased after IV administration of Ab-02 (Fig. 5A and B). The decrease in free IL-13 appeared more dramatic in Ascaris-challenged monkeys, because of the higher Ab-02 dose (10 mg/kg) used, relative to naive monkeys (1 mg/kg). In the Ascaris-challenge monkeys (Study 2), free IL-13 concentrations were predicted to remain at or below the estimate of free IL-13 concentrations in naive monkeys (i.e. below 0.0115 nM) for ~35 days post 10 mg/kg single IV administration of Ab-02. Free IL-13 concentrations in Ascaris-challenged monkeys were predicted to rise above the naive baseline average when Ab-02 concentration was ~160 nM. Along with the elimination of Ab-02, free IL-13 concentrations in naive and Ascaris-challenged monkeys gradually rose to the corresponding baseline concentrations (defined by $k_{syn}/CL_{IL\text{-}13}$).

The kinetics of IL-13 neutralization was also simulated with the different IV doses of Ab-02 (1–50 mg/kg) in monkeys with a hypothetic established airway inflammation, i.e. assuming Ascaris challenge at Day 0. Predicted free IL-13 concentrations in naive monkeys and in monkeys with established airway inflammation after a single IV administration of Ab-02 are shown in Fig. 6. In both naive monkeys and in monkeys with established airway inflammation, the time at which free IL-13 concentrations were below baseline IL-13 concentrations increased with the Ab-02 dosage used for the simulations. However, the extent and duration of IL-13 neutralization by Ab-02 appeared to differ between the naive monkeys and the monkeys with established airway inflammation. For example, after the 10-mg/kg IV dosage of Ab-02 to naive monkeys, most of the IL-13 appeared to be Ab-02-bound as late as Day 40 post-dose, with free IL-13 concentrations of <0.001 nM (or <7% of baseline). In contrast, after 10-mg/kg IV dosage of Ab-02 to monkeys with established airway inflammation, there was an initial drop in free IL-13 to nearly-zero concentrations followed by a steady rise to ~0.008 nM or 21% of baseline at Day 40.

DISCUSSION

In this report, we developed an integrated antibody–ligand binding PK–PD model that described the relationship between the total serum concentrations of IL-13 and Ab-02, an anti-IL-13 humanized IgG1 antibody, in naive cynomolgus monkeys and in the disease model of acute airway inflammation induced by Ascaris challenge to cynomolgus monkeys. Due to lack of a bioanalytical method of sufficient sensitivity, free IL-13 concentrations could not be directly measured in

Table II. Summary of Ab-02 Pharmacokinetic and Pharmacodynamic Parameters from Individual Fittings of Data for Naive and Ascaris-Challenged Cynomolgus Monkeys

	Naive monkeys		Ascaris-challenged monkeys	
	Mean ± SD (N=5)[a]	%CV	Mean ± SD (N=8)	%CV
CL_{Ab} (L day^{-1})	0.0148±0.0022	15	0.0130±0.0046	35
V (L)	0.222±0.045	20	0.145±0.048*	33
$CL_{d,Ab}$ (L day^{-1})	0.1877±0.1840	98	0.0238±0.0192*	81
V_2 (L)	0.136±0.071	53	0.111±0.058	22
k_{on} nM^{-1} day^{-1}	0.0896±0.0917	102	Fixed	NA
k_{off} (day^{-1})	0.1630±0.0959	59	Fixed	NA
$CL_{complex}$ (L day^{-1})	0.0024±0.0006	23	0.0097±0.0073*	75
k_{syn}/CL_{IL-13} (nM)	0.0115±0.0055	47	0.0346±0.0101**	29

[a] For estimation of mean parameters in naive animals, three animals in the 1 mg/kg, IV group and two animals in the 2 mg/kg, SC group were used. One animal in the SC group was excluded from calculations of mean parameters due to a sharp decline in Ab-02 concentrations (and total IL-13 concentrations) in the terminal phase, compared to other naive monkeys in the study

*$p \le 0.05$; **$p \le 0.001$ (indicate that a mean parameter in the Ascaris-challenged animals was significantly different from a corresponding value in naive monkeys, based on unpaired Student t test)

either the presence or the absence of Ab-02. Therefore, total IL-13 concentrations were used as a PD marker, as total IL-13 concentrations were transiently increased in both naive and Ascaris-challenged monkeys. The model presented in this report was developed under the assumption that Ab-02 can bind either one or two IL-13 molecules, in a sequential manner. Furthermore, non-cooperative binding for the two IgG binding sites was assumed, so that k_{on} and k_{off} rate constants were assumed to be identical for the first and the second binding steps. The above assumptions are based on the physiological mechanism of an antibody/antigen interaction and are different from those used in the previously published integrated antibody–ligand binding PK–PD models for therapeutic antibodies, in which either 1:1 or 1:2 stochiometry was assumed (21–25). The sequential binding models to describe antibody–antigen interactions in solution have been described previously for a variety of biochemical studies (26,27). The second main assumption of the current model is that the homeostasis of IL-13 is regulated by the zero-order synthesis and the first order degradation of IL-13. This assumption has been used in a number of published integrated PK–PD models for protein or small molecule therapeutics (21–25,28). In addition to the current sequential binding PK-PD model, two stochiometry binding models (in which either 1:1 or 1:2 stochiometry has been assumed) were also fitted to PK-PD profiles of Ab-02 during the initial model selection stage. The sequential PK/PD model was overall superior to the stochiometry binding models in describing the experimental data of IL-13 neutralization by Ab-02 in monkeys (data not shown).

The Ab-02 PK parameters estimated by PK-PD modeling were consistent with those estimated by non-compartmental analysis (20). Ab-02 had a low clearance and a small volume of distribution in monkeys, typical of those seen for other humanized IgG1 therapeutic proteins (29–31). The PK-PD modeling further confirmed that Ab-02 volume of distribution was smaller in Ascaris-challenged monkeys when compared

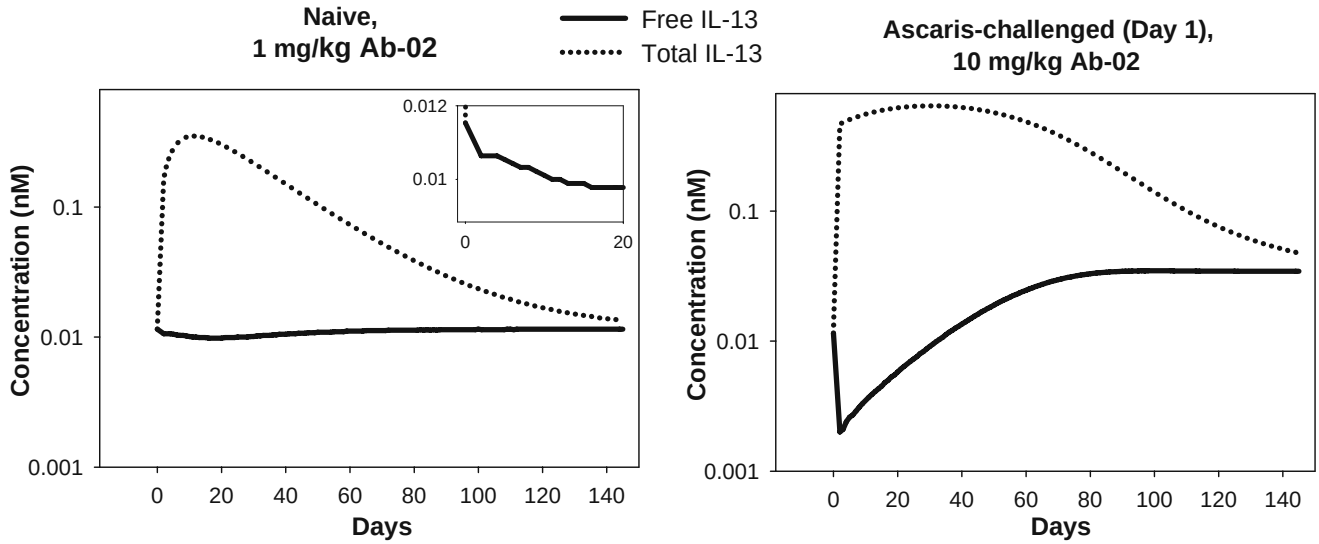

Fig. 5. Simulated free IL-13 and total IL-13 concentration-time profiles after a single IV administration of Ab-02 to cynomolgus monkeys. For naive monkeys, a 1 mg/kg dosage was assumed as in Study 1, while for Ascaris-challenged monkeys, a 10 mg/kg dosage and Ascaris challenge 24-h post Ab-02 administration (Day 1) were assumed as in Study 2. Free IL-13 is shown by *solid lines*, while total IL-13 is shown by *dotted lines*.

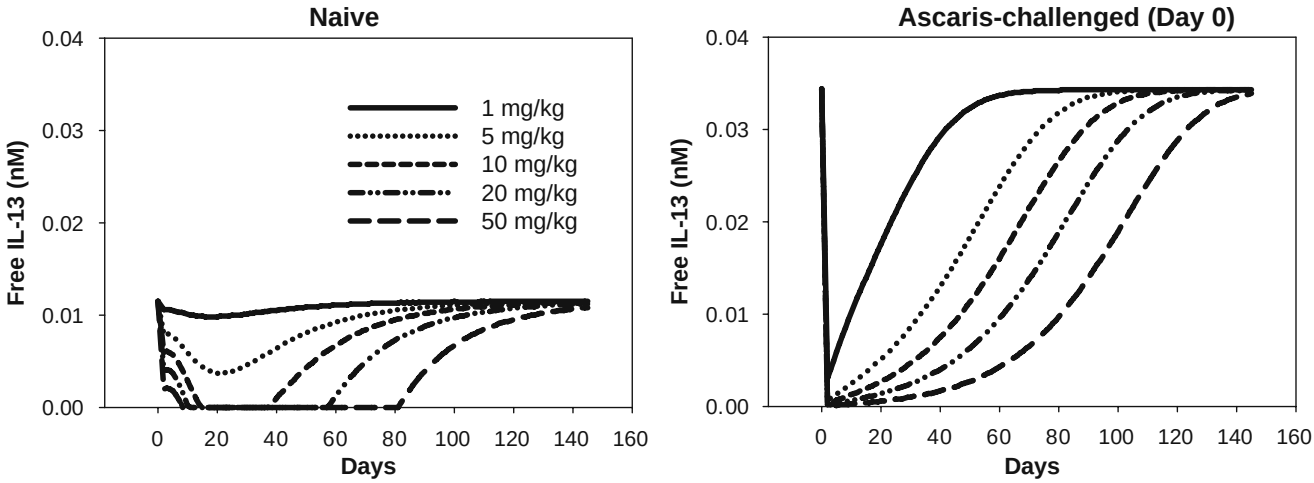

Fig. 6. Simulated free IL-13 concentration-time profiles after different dosing regimens of Ab-02 to cynomolgus monkeys. A single 1, 5, 10, 20, or 50 mg/kg IV bolus dosage of Ab-02 (as indicated) was assumed for both naive and Ascaris-challenged monkeys. Ascaris challenge was assumed at pre-dose (Day 0) to mimic the "established airway inflammation" situation.

to that in naive monkeys, in line with the results of non-compartmental analysis. Volume of distribution of Ab-02 in the central (V) and, to some degree, the peripheral (V_2) compartments, as well as the distribution clearance ($CL_{d,Ab}$) of Ab-02 between these two compartments were decreased in Ascaris-challenged monkeys when compared to those in naive monkeys. The difference of Ab-02 volume of distribution between naive and Ascaris-challenged monkeys was not likely due to the difference in Ab-02 dosage used (1 or 2 mg/kg in naive monkey and 10 mg/kg in Ascaris-challenged monkeys), since the steady-state volume of distribution (Vd_{ss}) of Ab-02, as estimated by the non-compartmental method, was similar among naive monkeys over a wide dose range (1–100 mg/kg) (20).

For both naive and Ascaris-challenged monkeys, the model also demonstrated that the transient increase in total IL-13 concentrations in Ascaris-challenged and naive animals was due to the increase in Ab-02-bound IL-13, while free IL-13 was decreased. The neutralization of IL-13 leading to decrease in free IL-13 concentrations is the intended biological effect of Ab-02 and is consistent with the observed efficacy of Ab-02 in reducing airway inflammation in the Ascaris-challenged animals, as well as with the lack of IL-13-mediated biological activity in the sera obtained from these animals (19).

Results of the PK–PD modeling and simulations indicated a number of differences in IL-13 neutralization between the naive and Ascaris-challenge settings. In the Ascaris-challenged animals, baseline IL-13 concentrations were estimated be ~ three-fold higher, when compared to those in naive monkeys. This estimation was consistent with the notion that acute airway inflammation induced by Ascaris challenge in cynomolgus monkeys was mediated by IL-13. In human subjects, including normal human volunteers and subjects with a variety of disorders, there is a wide range of reported baseline IL-13 concentrations (from <10 to >150 pg/mL), in part dependent on assay methodology employed for the measurements (32,33). In general, baseline IL-13 concentrations estimated for naive monkeys (~100 pg/mL or ~0.01 nM) appeared to be higher, compared to those reported for healthy humans.

In Ascaris-challenged animals (Study 2), free circulating IL-13 concentrations were maintained below the average free IL-13 concentrations in naive monkeys for ~1 month after a 10 mg/kg IV administration of Ab-02. Modeling and simulations indicated that for a given dose of Ab-02, extent and duration of Ab-02-mediated IL-13 neutralization in the naive and Ascaris-challenged monkeys were different. Thus, caution should be used when applying PK–PD data from normal human volunteers to the design of clinical studies in subjects with airway inflammation.

It should be noted that the concentrations of free IL-13 in the target tissue (lung) may be a more direct indicator of effectiveness of IL-13 neutralization by a therapeutic protein. However, the concentration at which tissue (and circulating) IL-13 needs to be maintained to suppress Ascaris-induced airway inflammation in monkeys (and in asthmatic patients), as well as the required duration of the neutralization, are not known. Total IL-13 concentrations were below the limit of detection in BAL (bronchoalveolar lavage) fluid of animals in Study 2 (data not shown), so that it was not possible to obtain a PD readout in the tissue compartment. In current modeling approach the combination of efficacious dose level data (10 mg/kg) and PK–PD modeling of serum data was used to predict the duration and extent of serum IL-13 neutralization that correlated with Ab-02 efficacy. Peripheral compartments can be added to describe the IL-13 neutralization process in tissues when more sensitive technology to detect tissue IL-13 levels is developed in the future.

The nature of therapeutic protein/ligand interaction should be taken into account when applying this model to bivalent protein based therapeutics (such as an antibody). For example, PK–PD interactions between a protein therapeutic and a multivalent ligand (i.e. an antigen that has more than one antigenic determinant) or a ligand that displays cooperative binding to a bivalent therapeutic protein (resulting in different k_{on} and/or k_{off} for the first and second steps) may not be adequately described by the sequential or stochiometry binding models. Physiological processes governing ligand homeostasis should also be considered before applying the current (and the previously published) models. The assumption that the apparent k_{syn} is the zero-order rate constant may

not hold for more complicated ligand production process, including feedback mechanisms or diurnal changes for the rate of ligand production (34).

CONCLUSIONS

In this report, we developed a novel PK–PD model that described the relationship between the total serum concentrations of IL-13 and Ab-02, an anti-IL-13 humanized IgG1 antibody, in naive and Ascaris-challenged monkeys. The modeling predictions were the following: (1) The estimated circulating IL-13 concentrations were increased ~ three-fold after the Ascaris-challenge, consistent with the notion that Ascaris-induced acute airway inflammation was IL-13-mediated. (2) The transient increase in total IL-13 concentrations observed in both naive and Ascaris-challenged monkeys following Ab-02 administration, was due to the increase in Ab-02-bound IL-13, while free IL-13 was decreased after IV administration of Ab-02. (3) When identical Ab-02 dose regimens were used for simulations, the extent and duration of IL-13 neutralization in the circulation were different in naive and airway inflammation settings. However, this prediction needs to be interpreted with caution, as the model does not describe neutralization of IL-13 in the lung, the target organ. The PK–PD model presented in this report may be applied to study drug–ligand interactions for other therapeutics proteins, in cases when free ligand (such as a cytokine) cannot be directly assayed but total ligand concentrations change with drug administration. However, the nature of drug/ligand interactions, as well as physiologically processes governing ligand homeostasis should be considered before applying the model. The differences in the ligand neutralization by a therapeutic protein between the healthy and pharmacology-model settings described in this report, illustrate the importance of conducting preclinical PK-PD studies in both settings, if practically feasible.

ACKNOWLEDGMENTS

We thank Macy Jin, Xiang-Yang Tan, and Lioudmila Tchistiakova for generation and humanization of Ab-02; Tamera Ashworth, Nicole Duriga, Nick Bauer, and David DeFranco for technical help with bioanalytical aspects of the studies; Andrea Bree, Franklin Schlerman, and Michael Wadanoli for help with Ascaris challenge studies in monkeys; Vikram Patel, Joann Scatina, Qin Wang, Mauricio Leal, Stan Spence, and Garvin Warner for scientific discussions on data interpretation.

REFERENCES

1. J. H. Anolik, and M. Aringer. New treatments for SLE: cell-depleting and anti-cytokine therapies. *Best Pract. Res. Clin. Rheumatol.* **19**(5):859–878 (2005) doi:10.1016/j.berh.2005.05.006.
2. A. N. Economides, L. R. Carpenter, J. S. Rudge, V. Wong, E. M. Koehler-Stec, C. Hartnett *et al.* Cytokine traps: multi-component, high-affinity blockers of cytokine action. *Nat. Med.* **9**(1):47–52 (2003) doi:10.1038/nm811.
3. E. Toussirot, and D. Wendling. The use of TNF-alpha blocking agents in rheumatoid arthritis: an update. *Expert Opin. Pharmacother.* **8**(13):2089–2107 (2007) doi:10.1517/14656566.8.13.2089.
4. M. Ichinose, and P. J. Barnes. Cytokine-directed therapy in asthma. *Curr. Drug Targets Inflamm. Allergy*. **3**(3):263–269 (2004) doi:10.2174/1568010043343688.
5. K. Margolin, M. S. Gordon, E. Holmgren, J. Gaudreault, W. Novotny, G. Fyfe *et al.* Phase Ib trial of intravenous recombinant humanized monoclonal antibody to vascular endothelial growth factor in combination with chemotherapy in patients with advanced cancer: pharmacologic and long-term safety data. *J. Clin. Oncol.* **19**(3):851–856 (2001).
6. H. Ito, M. Takazoe, Y. Fukuda, T. Hibi, K. Kusugami, A. Andoh *et al.* A pilot randomized trial of a human anti-interleukin-6 receptor monoclonal antibody in active Crohn's disease. *Gastroenterology*. **126**(4):989–996 (2004)discussion 947 doi:10.1053/j.gastro.2004.01.012.
7. P. Charles, M. J. Elliott, D. Davis, A. Potter, J. R. Kalden, C. Antoni *et al.* Regulation of cytokines, cytokine inhibitors, and acute-phase proteins following anti-TNF-alpha therapy in rheumatoid arthritis. *J. Immunol.* **163**(3):1521–1528 (1999).
8. A. L. Andrews, J. W. Holloway, S. M. Puddicombe, S. T. Holgate, and D. E. Davies. Kinetic analysis of the interleukin-13 receptor complex. *J. Biol. Chem.* **277**(48):46073–46078 (2002) doi:10.1074/jbc.M209560200.
9. D. B. Corry, and F. Kheradmand. Biology and therapeutic potential of the interleukin-4/interleukin-13 signaling pathway in asthma. *Am. J. Respir. Med.* **1**(3):185–193 (2002).
10. M. Wills-Karp. Interleukin-13 in asthma pathogenesis. *Curr. Allergy Asthma Rep.* **4**(2):123–131 (2004) doi:10.1007/s11882-004-0057-6.
11. C. Taube, C. Duez, Z. H. Cui, K. Takeda, Y. H. Rha, J. W. Park *et al.* The role of IL-13 in established allergic airway disease. *J. Immunol.* **169**(11):6482–6489 (2002).
12. J. Padilla, E. Daley, A. Chow, K. Robinson, K. Parthasarathi, A. N. McKenzie *et al.* IL-13 regulates the immune response to inhaled antigens. *J. Immunol.* **174**(12):8097–8105 (2005).
13. G. Grunig, M. Warnock, A. E. Wakil, R. Venkayya, F. Brombacher, D. M. Rennick *et al.* Requirement for IL-13 independently of IL-4 in experimental asthma. *Science*. **282**(5397):2261–2263 (1998) doi:10.1126/science.282.5397.2261.
14. D. Vercelli. Genetics of IL-13 and functional relevance of IL-13 variants. *Curr. Opin. Allergy Clin. Immunol.* **2**(5):389–393 (2002) doi:10.1097/00130832-200210000-00004.
15. R. K. Kumar, C. Herbert, D. C. Webb, L. Li, and P. S. Foster. Effects of anticytokine therapy in a mouse model of chronic asthma. *Am. J. Respir. Crit. Care Med.* **170**(10):1043–1048 (2004) doi:10.1164/rccm.200405-681OC.
16. G. Yang, L. Li, A. Volk, E. Emmell, T. Petley, J. Giles-Komar et al. Therapeutic dosing with anti-interleukin-13 monoclonal antibody inhibits asthma progression in mice. *J. Pharmacol. Exp. Ther.* **313**(1):8–15 (2005) doi:10.1124/jpet.104.076133.
17. M. Wills-Karp, J. Luyimbazi, X. Xu, B. Schofield, T. Y. Neben, C. L. Karp *et al.* Interleukin-13: central mediator of allergic asthma. *Science*. **282**(5397):2258–2261 (1998) doi:10.1126/science.282.5397.2258.
18. A. Bree, F. J. Schlerman, M. Wadanoli, L. Tchistiakova, K. Marquette, X. Y. Tan *et al.* IL-13 blockade reduces lung inflammation after Ascaris suum challenge in cynomolgus monkeys. *J. Allergy Clin. Immunol.* **119**(5):1251–1257 (2007) doi:10.1016/j.jaci.2007.02.009.
19. M. T. Kasaian, X. Y. Tan, M. Jin, L. Fitz, K. Marquette, N. Wood, *et al.* IL-13 Neutralization by two distinct receptor blocking mechanisms reduces IgE responses and lung inflammation in cynomolgus monkeys. *J. Pharmacol. Exp. Ther.* **325**(3):88 (2008).
20. Y. Vugmeyster, P. Szklut, L. Tchistiakova, W. Abraham, M. Kasaian, and X. Xu. Preclinical pharmacokinetics, interspecies scaling, and tissue distribution of humanized monoclonal anti-IL-13 antibodies with different IL-13 neutralization mechanisms. *Int. Immunopharmacol.* **8**(3):477–483 (2008) doi:10.1016/j.intimp.2007.12.004.
21. L. J. Benincosa, F. S. Chow, L. P. Tobia, D. C. Kwok, C. B. Davis, and W. J. Jusko. Pharmacokinetics and pharmacodynamics of a humanized monoclonal antibody to factor IX in cynomolgus monkeys. *J. Pharmacol. Exp. Ther.* **292**(2):810–816 (2000).

22. D. E. Mager, and W. J. Jusko. General pharmacokinetic model for drugs exhibiting target-mediated drug disposition. *J. Pharmacokinet. Pharmacodyn.* **28**(6):507–532 (2001) doi:10.1023/A:1014414520282.
23. C. M. Ng, E. Stefanich, B. S. Anand, P. J. Fielder, and L. Vaickus. Pharmacokinetics/pharmacodynamics of nondepleting anti-CD4 monoclonal antibody (TRX1) in healthy human volunteers. *Pharm. Res.* **23**(1):95–103 (2006) doi:10.1007/s11095-005-8814-3.
24. F. S. Chow, L. J. Benincosa, S. B. Sheth, D. Wilson, C. B. Davis, E. A. Minthorn *et al.* Pharmacokinetic and pharmacodynamic modeling of humanized anti-factor IX antibody (SB 249417) in humans. *Clin. Pharmacol. Ther.* **71**(4):235–245 (2002) doi:10.1067/mcp.2002.122276.
25. N. Hayashi, Y. Tsukamoto, W. M. Sallas, and P. J. Lowe. A mechanism-based binding model for the population pharmacokinetics and pharmacodynamics of omalizumab. *Br. J. Clin. Pharmacol.* **63**(5):548–561 (2007) doi:10.1111/j.1365-2125.2006.02803.x.
26. K. M. Muller, K. M. Arndt, and A. Pluckthun. Model and simulation of multivalent binding to fixed ligands. *Anal. Biochem.* **261**(2):149–158 (1998) doi:10.1006/abio.1998.2725.
27. W. L. Tseng, H. T. Chang, S. M. Hsu, R. J. Chen, and S. Lin. Immunoaffinity capillary electrophoresis: determination of binding constant and stoichiometry for antibody–antigen interaction. *Electrophoresis*. **23**(6):836–846 (2002) doi:10.1002/1522-2683(200203)23:6<836::AID-ELPS836>3.0.CO;2-J.
28. M. Danhof, J. de Jongh, E. C. De Lange, O. Della Pasqua, B. A. Ploeger, and R. A. Voskuyl. Mechanism-based pharmacokinetic–pharmacodynamic modeling: biophase distribution, receptor theory, and dynamical systems analysis. *Annu. Rev. Pharmacol. Toxicol.* **47**:357–400 (2007) doi:10.1146/annurev.pharmtox.47.120505.105154.
29. C. W. Adams, D. E. Allison, K. Flagella, L. Presta, J. Clarke, N. Dybdal *et al.* Humanization of a recombinant monoclonal antibody to produce a therapeutic HER dimerization inhibitor, pertuzumab. *Cancer Immunol. Immunother.* **55**(6):717–727 (2006) doi:10.1007/s00262-005-0058-x.
30. Y. S. Lin, C. Nguyen, J. L. Mendoza, E. Escandon, D. Fei, Y. G. Meng *et al.* Preclinical pharmacokinetics, interspecies scaling, and tissue distribution of a humanized monoclonal antibody against vascular endothelial growth factor. *J. Pharmacol. Exp. Ther.* **288**(1):371–378 (1999).
31. P. Zia-Amirhosseini, E. Minthorn, L. J. Benincosa, T. K. Hart, C. S. Hottenstein, L. A. Tobia *et al.* Pharmacokinetics and pharmacodynamics of SB-240563, a humanized monoclonal antibody directed to human interleukin-5, in monkeys. *J. Pharmacol. Exp. Ther.* **291**(3):1060–1067 (1999).
32. P. Fiumara, F. Cabanillas, and A. Younes. Interleukin-13 levels in serum from patients with Hodgkin disease and healthy volunteers. *Blood*. **98**(9):2877–2878 (2001) doi:10.1182/blood.V98.9.2877.
33. S. M. Wang, H. Y. Lei, M. C. Huang, L. Y. Su, H. C. Lin, C. K. Yu *et al.* Modulation of cytokine production by intravenous immunoglobulin in patients with enterovirus 71-associated brainstem encephalitis. *J. Clin. Virol.* **37**(1):47–52 (2006) doi:10.1016/j.jcv.2006.05.009.
34. J. Gabrielsson, and D. Weiner. Pharmacokinetic and pharmacodynamic data analysis: concept and applications. Swedish Pharmaceutical, Stockholm, 2000.